Petroleum 11 (2025) 366–376

Contents lists available at ScienceDirect

Petroleum

journal homepage: www.keaipublishing.com/en/journals/petlm

Full Length Article

An experimental study to investigate the role of pyrolysis reaction on in-situ hydrogen generation from sandstone oil reservoirs

Mohamed Abdalsalam Hanfi [a], Olalekan Saheed Alade [b], Abdulkadir Tanimu [c], Mohamed Mahmoud [a], Sulaiman A. Alarifi [a, *]

[a] Department of Petroleum Engineering, King Fahd University of Petroleum & Minerals (KFUPM), Dhahran, 31261, Saudi Arabia
[b] Center for Integrative Petroleum Research (CIPR), King Fahd University of Petroleum & Minerals, Dhahran, 31261, Saudi Arabia
[c] Interdisciplinary Research Center for Refining and Advanced Chemicals, Research Institute, King Fahd University of Petroleum and Minerals, Dhahran 31261, Saudi Arabia

ARTICLE INFO

Article history:
Received 4 November 2024
Received in revised form
9 December 2024
Accepted 7 May 2025

Keywords:
Hydrogen generation
Crude oil
In-situ pyrolysis
Sandstone mineralogy
Pyrolysis products

ABSTRACT

In-situ combustion gasification (ISCG) is a technology in the field pilot stage used for hydrogen generation from oil reservoirs. ISCG is implemented by injecting an oxidant (pure oxygen, air, …) into the reservoir to trigger in-situ chemical reactions responsible for hydrogen generation. Pyrolysis reaction is one of the significant reactions triggered by in-situ combustion (ISC). This study used a fixed-bed micro-activity test (MAT) unit to investigate hydrogen generation from crude oil through pyrolysis. Crude oil pyrolysis experiments were conducted in the MAT unit under different temperatures (300 °C, 400 °C, 500 °C, 600 °C), atmospheric pressure, and under a flow of a nitrogen gas. The results showed that the threshold initiation temperature of hydrogen generation and coke formation was about 500 °C. The experiments demonstrated that the introduced sandstone enhanced hydrogen generation and coke formation at high temperatures. The maximum volume of hydrogen generated with sandstone effect reached 8.15 mL at 600 °C, while that without sandstone was only 6.39 mL at 600 °C. The study provides deep insights into the in-situ hydrogen generation from crude oil through pyrolysis. In addition, the obtained data of various pyrolysis products provide a comprehensive representation of crude oil pyrolysis that could promote the existing reaction models of in-situ hydrogen generation from the gasification of crude oil. The findings demonstrate the potential of adopting pyrolysis of crude oil for direct hydrogen generation from reservoirs.

1. Introduction

The global energy scene is currently experiencing a noteworthy transformation, driven by the global effort to address climate change and improve energy security. Hydrogen (H_2) is hailed as a clean energy carrier that contributes to sustainable energy development and mitigation of climate change problems [1]. Various renewable sources (such as solar and wind) and non-renewable sources (like nuclear and fossil fuels) can be utilized for hydrogen generation [2]. It has been demonstrated that fossil fuels, especially natural gas are the most utilized source for generating hydrogen through various reactions such as water gas shift reaction, partial oxidation, and steam reforming [2,3]. Due to the considerable amount of carbon dioxide emitted from utilizing fossil fuels in hydrogen generation [4], in-situ hydrogen generation from heavy oil was proposed to exploit the considerable amount of unrecoverable oil in the reservoirs [5,6]. It has been reported that hydrogen can be generated from in-situ hydrocarbon reservoirs by converting unrecoverable oil into pure hydrogen gas using the in-situ combustion gasification (ISCG) method that relies on a series of parallel or separate reactions (pyrolysis, water-gas shift reaction, partial oxidation, coke gasification) between crude oil, water, and reservoir rocks at elevated temperatures [7]. ISCG involves heating the crude oil in the reservoir by implementing in-situ combustion that initiates a series of gasification reactions that result in the generation of a hydrogen-rich gas mixture. A selective hydrogen membrane can separate the generated hydrogen placed downhole while the

* Corresponding author.
E-mail address: salarifi@kfupm.edu.sa (S.A. Alarifi).
Peer review under the responsibility of Southwest Petroleum University.

https://doi.org/10.1016/j.petlm.2025.05.002

unwanted gases (carbon dioxide) are left in the reservoir. In-situ combustion (ISC) involves creating a combustion front by injecting an oxidant into the reservoir and igniting part of the reservoir's oil. The combustion front provides the desired heat for the gasification process. Ahead of the combustion front the heat is transferred by conduction to the surrounding and fueling the combustion front with the formed coke.

Pyrolysis is considered one of the reactions that take place in the reservoir during the ISCG process. It is also known as thermolysis and thermal cracking which is defined as the thermal decomposition of crude oil in a free-oxygen environment. In general, the pyrolysis reaction can be divided into two stages. The first stage comprises dehydrogenation, dehydration, and decarboxylation. While the second stage involves cracking of the heavy components to give gas products, liquid products, and coke as solid products. On the other hand, pyrolysis reaction can be classified as flash, fast, intermediate, or slow based on the heating rate and residence time [8]. Liu et al. conducted a pyrolysis experiment of Indonesian oil sand using a fixed bed reactor at temperatures from 400 to 600 °C. They found that as the temperature increases, the gases and the condensed liquid yield increase while the coke yield decreases. However, the generated gases are composed mainly of H_2, CH_4, C_2H_6, C_3H_8, and C_2H_4, with approximately 50% of the total volume being hydrogen gas [5,9–11]. Researchers conducted experimental studies on the hydrogen production from crude oil using various equipment, like a fixed-bed reactor, a thermogravimetric analyzer coupled to a mass spectrometer (TGA-MS), and a kinetic cell. Previous studies conducted on heavy oil upgrading revealed that the thermal cracking of crude oil under high temperatures and in the absence of oxygen produces more gases [12,13].

Yang et al. [14] utilized TGA-MS to study the mechanisms involved in the hydrogen generation from heavy oil pyrolysis and they define two stages (physical and chemical stages) in which weight loss occurred. They also stated that a higher percentage of the hydrogen is generated from coke dehydrogenation, while around 20% comes from pyrolysis reaction. Tang et al. studied hydrogen generation for heavy and light oil using TGA-MS combined with equivalent characteristic spectrum analysis (ECSA). It was found that hydrogen was mainly generated during the pyrolysis stage in the temperature range of 358–521 °C [15]. Zhao et al. conducted experiments on heavy oil using a kinetic cell to investigate in-situ hydrogen generation. The results revealed that pyrolysis and coke dehydrogenation reactions generated hydrogen under a nitrogen environment, with 60% of the total hydrogen generated by the coke dehydrogenation reaction in the temperature range of 500–650 °C [10]. He et al. experimentally mimics the oxidation reaction of heavy oil, light oil, and carbon samples to investigate hydrogen generation using a ramped temperature oxidation device. The experimental design comprised sand fill and reservoir core models. The results revealed that hydrogen generation was observed at a temperature range of 500–550 °C whereas that of carbon fell in the range of 700–750 °C. The reservoir core produced hydrogen with a maximum rate of 55–60 mol%, while hydrogen production from sand-filling experiments reached only 5–10 mol% [16]. Yuan et al. investigated the hydrogen generation from a mixture of crude oils, rock powders, catalysts, and water using a quartz tube reactor and microwave generation system. The results showed that the maximum hydrogen production was 197 mL, obtained from heating the mixture at 354 °C for a reaction time of 47 minutes [17].

Implementation of in-situ combustion has been reported for different crude oil reservoirs. The feasibility of upscaling the ISCG laboratory experiments to field scale can be confirmed from the temperature profiles reported in the literature for many in-situ combustion field projects [18]. The Nacatoch sand reservoir with a thin column of heavy crude oil with 20.9 °API gravity was selected for the thermal recovery process. Harrell Fee in-situ combustion project was initiated in 1980. The project reported that the formation temperature during ignition in the combustion zone reached 1000 °F after 9 hours of ignition. In 1984, an O_2 combustion pilot test was conducted in the Miocene I sand body at the Esperson Dome field. The reservoir oil has a gravity of 21 °API. The results obtained from the X-ray diffraction (XRD) indicated that the temperature in the combustion zone was in the range between 930 °F and 1020 °F [19]. In 1970, Bayou State Oil Corp. (BSOC) initiated the ISC project in Nacatoch formation in the Bellevue field in Louisiana, one of the remaining active firefloods worldwide. The oil has a 19°API gravity. The reported ignition temperature was approximately 500 °F. Temperature surveys taken by wireline in the injection periodically showed that the temperature exceeded 800 °F [20].

It can be inferred from the preceding reports show that various thermochemical reactions, including pyrolysis play a crucial role in the hydrogen generation process. However, each reaction's contribution and importance, especially pyrolysis, are still not adequately understood. In addition, there is a contradiction in these reported studies regarding whether the saturate, aromatics, resin, and asphaltene (SARA) fractions of crude oil contribute more to the gases generated by cracking [21–23].

In this paper, a fixed-bed micro-activity test (MAT) unit was used to study the quantitative and qualitative characteristics of various pyrolysis products, especially the generated hydrogen gas. Furthermore, the effect of sandstone mineralogy on the pyrolysis reaction was studied by introducing crushed sandstone rock. The direct collection of various pyrolysis products without post-processing gives this work an advantage over existing experimental studies in the literature. The detailed results of the pyrolysis products provide powerful data for kinetic model development. Furthermore, the results provide deep insights for future research on in-situ hydrogen generation from crude oil.

2. Materials and method

2.1. Materials

2.1.1. Crude oil sample

The oil sample used in this study was obtained from an oil field in Saudi Arabia. The results of density, viscosity and elemental analysis, distillation cuts are shown in Table 1. SARA fractions were measured for the original crude oil sample as shown in Fig. 1.

2.1.2. Sandstone rock samples

Dried, crushed sandstone was introduced during the pyrolysis reaction to study the effect of sandstone mineralogy on both pyrolysis reaction and hydrogen generation. Berea sandstone was

Table 1
Viscosity, density, distillation cuts, and elemental analysis of crude oil sample.

Parameter	Value
Viscosity at 22.8 °C (cP)	91.6
Density at 21 °C (g/cm^3)	0.907
API (°)	24.0
Elemental analysis (wt.%)	
C	84.1
H	11.3
N	0
S	1.3
Distillation cuts (wt.%)	
Gasoline (0–221 °C)	35.4
Light cycle oil (LCO: 221–343 °C)	25.1
Heavy cycle oil (HCO: >343 °C)	39.6

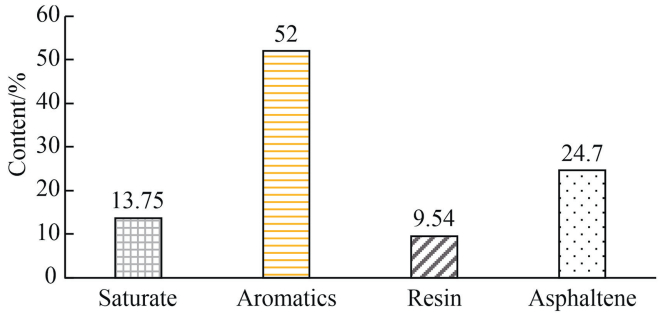

Fig. 1. SARA fractions of crude oil sample.

procured from Kocurek Industries. The mineral composition of the sandstone rock sample as analyzed by XRD is listed in Table 2. About 5 g of dried, crushed sandstone was loaded on top of the quartz wool placed at the bottom of the reactor of the MAT unit during the experiments to investigate the effect of sandstone on the pyrolysis reaction.

2.2. Pre and post-analytical measurements

Pyrolysis products were characterized using various analyzers including thin layer chromatography coupled with a flame ionization detector (TLC-FID) for SARA analysis of liquid products, gas chromatography coupled with a flame ionization detector (GC-FID) for simulated distillation analysis of liquid products according to ASTM 2887, gas chromatography coupled with thermal conductivity detector (GC-TCD) for gas product analysis according to the American Standard Society for Testing and Materials (ASTM) UOP539-97 refinery gas analysis method, CHNS elemental analysis for liquid products and coke, XRD for mineralogy of sandstone rock and Scanning electron microscopy (SEM) for the coke product.

2.2.1. Viscosity measurement

The viscosity of the crude oil was measured using a Viscolab PVT analyzer from Cambridge according to standard method ASTM D445, ASTM D7483.

2.2.2. Density measurement

The density of the crude oil was measured using a DMA 53 Handheld density meter from Anton Paar. Crude oil was injected into the measuring cell through a sampling tube. Direct reading was recorded from the instrument's screen.

2.2.3. X-ray diffraction (XRD)

The mineralogy of the sandstone powder was analyzed using an X-ray diffractometer (Miniflex, Rigaku). The diffraction pattern was measured in the range of 5–70° 2θ with Cu K-α as the radiation source (λ = 1.5418 Å).

Table 2
Mineral composition of sandstone rock sample.

Content	Concentration(wt.%)
Quartz	89.0
Calcite	0.08
Albite	1.47
Kaolinite	4.80
Illite	2.29
Chlorite	1.02
Ankertite	0.38

2.2.4. Scanning electron microscopy (SEM)

The coke samples were imaged using Zeiss Gemini 450 field-emission electron microscope (FE-SEM). The samples were scanned at a high resolution of up to 10 μm. The samples were first coated using a Leica EM AC 900. SEM images were acquired at an acceleration voltage of 5 kV and beam currents of 98 pA.

2.2.5. CHNS elemental analysis

The elemental analysis of the coke and liquid samples was conducted using EMA 502 elemental micro-analyzer from VELP Scientifica.

2.2.6. SARA analysis

The liquid samples were analyzed using Iatroscan MK-7 TLC-FID, according to the standard method IP 469/01. The SARA analysis was carried out in three stages: (1) spotting 1 μL of the sample diluted in dichloromethane in chromorode (quartz rod covered with silica), (2) elution of the spotted samples using thin-layer chromatography (TLC), and (3) detection of different groups along the chromarod using a flame ionization detector (FID).

2.2.7. Simulated distillation (SimDist) analysis

The liquid samples were analyzed using Shimadzu GC 2010 Plus coupled with a flame ionization detector according to the ASTM 2887.

2.2.8. Gas analysis

The gaseous products were analyzed using an Agilent 3000 A micro-GC coupled with a thermal conductivity detector. The analysis was performed using the ASTM UOP539-97 Refinery Gas Analysis (RGA) method. A standard gas mixture with a certain volume concentration percentage (vol%) of H_2 and C_1–C_6 hydrocarbon was used for the GC calibration.

2.3. Experimental setup and procedure

Pyrolysis experiments were conducted using a MAT unit, in which pyrolyzed products (gas, liquid, and coke) were collected directly and analyzed. The MAT unit consists of a feed syringe, feed nozzle, nitrogen line, reactor, reactor furnace, glass receiver, and water-filled graduated cylinder (Fig. 2). Before the pyrolysis experiment, the pyrolysis temperature was set at a specific temperature which was selected from four proposed temperatures 300, 400, 500 and 600 °C. The reactor was cleaned with solvent and dried, and then about 1 g of quartz wool was inserted at the bottom of the reactor. For the sandstone experiments, 5 g of crushed dried sandstone was loaded on top of the quartz wool, then followed by additional quartz wool. An automated syringe containing a known amount of crude oil was mounted to the feed nozzle of the MAT unit. The syringe was connected to the feed nozzle and nitrogen line through a three-way valve. The unit was kept under the flow of nitrogen before injecting the feed sample. The crude oil feed was injected for 30 seconds, and immediately after the injection, the three-way valve was switched to allow the flow of nitrogen into the feed nozzle. The nitrogen carries the cracked products (liquid and gas) down to the glass receiver, where the liquid products were condensed in a 2 mL vial connected to the glass receiver, and the gas products were collected in a water-filled graduated cylinder and their volume was measured by the water displacement. Then, the gas products were transferred to a Tedlar bag for injection into the GC-TCD. A standard gas mixture with a certain percent volume concentration (vol%) of H_2 and C_1–C_6 hydrocarbon was used for the GC calibration. Based on the peak area of the individual gas products, the vol% of the gas products was calculated. The vol% is converted to weight using the ideal gas equation. A total of eight

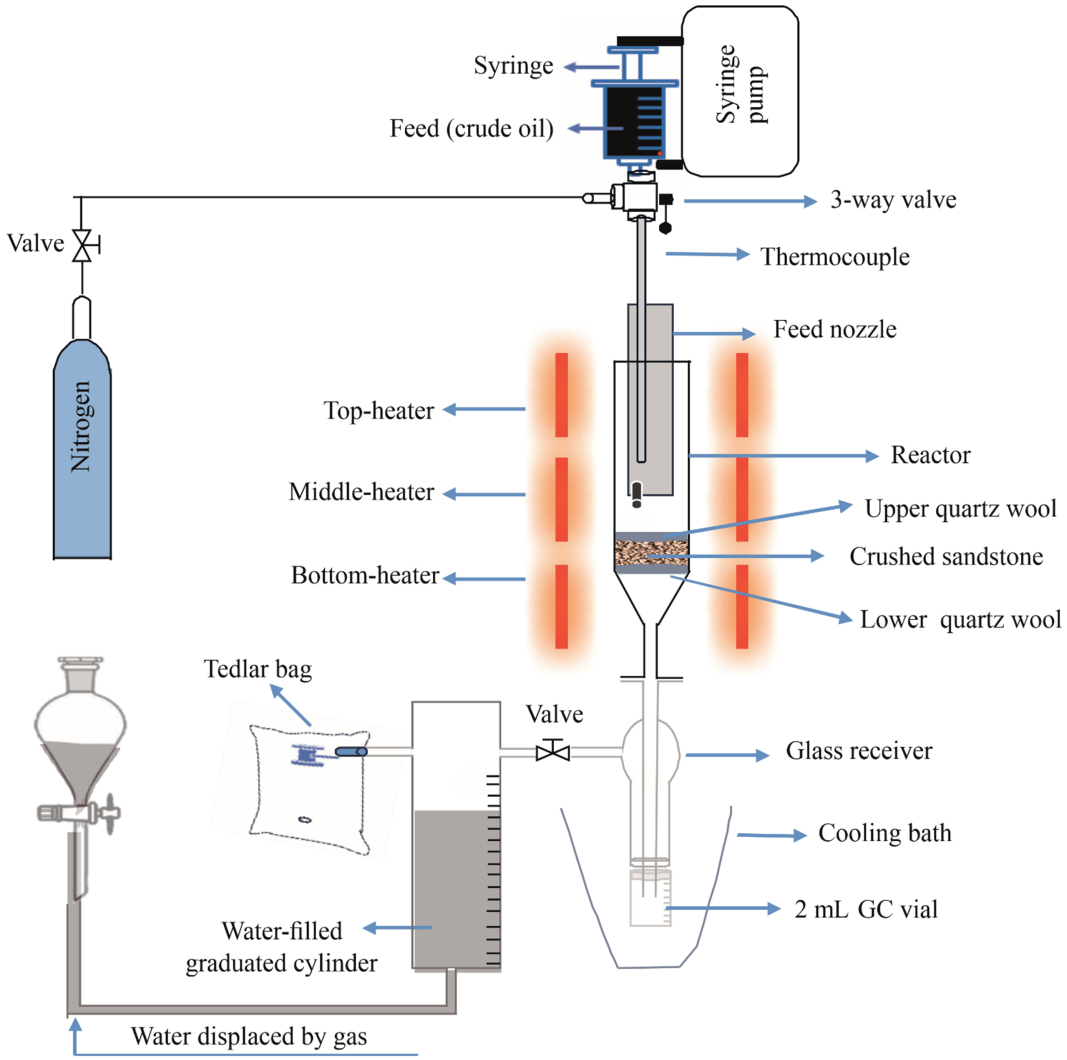

Fig. 2. Micro-activity test (MAT) unit.

experiments were conducted to investigate the contribution of pyrolysis reaction on the in-situ hydrogen generation from crude oil. Four experiments were conducted with crude oil only (section 3.1), while the other four were run with the presence of sandstone placed at the bottom of the reactor (Section 3.2). Uncertainty in the measurement equipment, loose pieces of coke while retrieved from the reactor, adhering of sticky heavy liquid to the reactor wall, and uncareful filling the syringe may result in uncertainty in estimation of feed weight.

3. Results and discussions

In these experiments, the products (gas, liquid, coke) of the crude oil pyrolysis were evaluated quantitively and qualitatively. The effect of pyrolysis temperature as well as the effect of dried crushed sandstone on the products was studied. This research investigates comprehensively the products of crude oil pyrolysis in general and specifically the hydrogen generated within the gas mixture.

3.1. Effect of pyrolysis temperature

Four different temperatures (600, 500, 400, and 300 °C) were applied during the pyrolysis experiment at atmospheric pressure. Each temperature represents a separate experiment conducted by injecting approximately 1 g of crude oil into the reactor. The types of pyrolysis products yield at each pyrolysis temperature are shown in Fig. 3. It was observed that at low temperatures, sticky heavy liquid product stuck to the surface of the quartz wool after the pyrolysis reaction. Specifically, at pyrolysis temperatures 300 °C and 400 °C, the yields of heavy liquid that stuck on the quartz wool were calculated as 49.7% and 34.6% of the total product yield, respectively. Similarly, the yields of condensed liquid products at temperatures of 300 °C and 400 °C are 49.6% and 64.5%, respectively, while the gaseous products were relatively minimal at both temperatures. It was also observed that no coke was produced at pyrolysis temperature below 500 °C. It is suspected that at these temperatures below 500 °C, the process resembles the visbreaking process. It is well known that the composition of crude oil intrinsically affects its thermal stability [24]. Hence, the distillation of the low boiling point components majorly contributes to the condensed liquid yield whilst the heavy components (resin and asphaltene) are suspected to be deposited as a sticky heavy liquid on the quartz wool. According to Fig. 3, the increase in temperature from 300 °C to 400 °C leads to an increase in the yields of the condensed liquid and a decrease in the yields of the sticky heavy liquid. This may be attributed to an enhancement of the thermal cracking process which is responsible for reducing the presence of

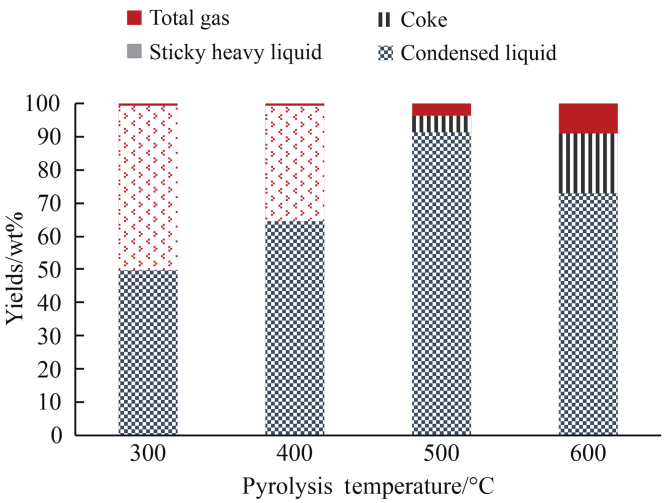

Fig. 3. Pyrolytic products yield at different pyrolysis temperatures.

heavy components and aiding in the further formation of low boiling point components that are present in the original sample. For high temperatures, the yield of gaseous products that was calculated as 3.62% at 500 °C increased to 8.94% at 600 °C. Additionally, about 4.94% coke was observed at 500 °C which increased consistently with increasing temperature to 18.8% at 600 °C. These observations imply that pyrolysis of crude oil at high temperatures of 500 and 600 °C is characterized by the formation of gaseous products and coke. High temperatures cause the decomposition of heavy components and larger hydrocarbons to generate more low molecular weight gaseous hydrocarbons. However, the formation of coke at higher temperatures is induced mainly by asphaltene since it is known as a direct precursor of coke due to its structural similarity [25].

It is seen from the results that a pyrolysis temperature of 500 °C is considered as the initiation threshold temperature of coking and hydrogen generation under atmospheric pressure and nitrogen environment. It is necessary to state that the heavy liquid stuck to the quartz wool cannot be retrieved so it was difficult to be sampled for further characterization while the coke was easily sampled and characterized.

3.1.1. Pyrolytic gas product

Fig. 4 shows the effect of pyrolysis temperature on the total volume of gas products produced at each experiment. The total volume of the gases included the sum of H_2, CH_4, C_2H_4, CO_2, CO, H_2S, and a sum of ($C_2 - C_4$) combination. It is clearly illustrated in (Fig. 4) that the volume of the gas produced increased exponentially with temperature from 1.92 mL/g at 300 °C to a maximum value of 74.04 mL/g at 600 °C. It was also observed that at low

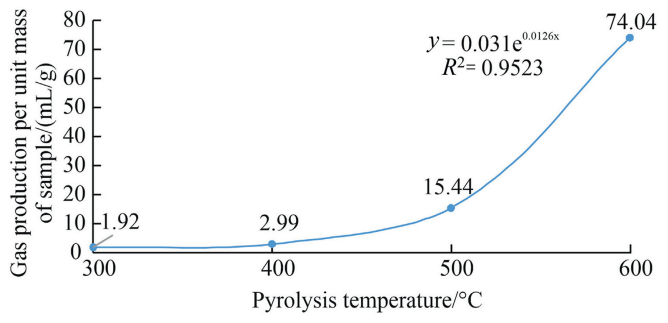

Fig. 4. Gas yield per unit mass of the crude oil sample.

temperatures a small amount of gas was produced due to the evolution of low volatile components and potential mild cracking of the heavy molecules in the crude oil during the pyrolysis. Whereas the noticeable increase in the total volume of gas at high temperatures was attributed mainly to the decomposition of the heavy components into gaseous hydrocarbons. Kapadia et al. [26] proposed a reaction scheme where asphaltenes as a pseudo-component can react and get converted into gases and other different components. In comparison with Kapadia's assumptions, it is suspected that the conversion of resins and asphaltene is affected by the pyrolysis temperature mainly and this is reflected in the observed enhancement in the total volume of gaseous products. On the other hand, the disappearance of the sticky heavy liquid accompanied by the appearance of the coke product and the increase in the generated gases at temperatures above 400 °C can be referred to as the conversion of heavy components, especially asphaltene.

The volume of various components of the gas products is tabulated in Table 3. At higher temperatures, the volume of the hydrogen gas ranked as the fifth most generated gas at 600 °C with volume of 6.39 mL. The generation of hydrogen is linked to the decomposition of heavier components into lighter unsaturated components, inferring the C—C, C—H, and H—H bond scissoring reactions. Moreover, the dehydrogenation of naphthenic rings present in the asphaltene can generate more hydrogen [27]. Similarly, CH_4, C_2H_4, C_3H_6, and C_2H_6 volumes rose dramatically reaching the highest values of 20.47, 15.24, 12, and 9.47 mL, respectively. The release of the high amount of methane is attributed to the C—C cleavages of cycloalkanes and alkyl side chains [28]. However, at lower temperatures of 300 and 400 °C only propane and *n*-butane show high volume compared to the other gas components. According to Wakui et al. [29], the propane is generated at the initial step of cracking and thus limits the generation of light ethylene and propylene. Also, they stated that cracking of dehydrogenated *n*-butane would increase the generation of ethylene. Here we can state that the efficiency of hydrogen generation through heavy components pyrolysis is affected by the formation of light-saturated hydrocarbons such as methane, ethane, and propane. In contrast, more efficient generation favored the formation of light unsaturated hydrocarbons ethylene and propylene.

3.1.2. Pyrolytic liquid product

The condensed liquid products were collected in a 2 mL vial after each experiment as shown in Fig. 5. It was observed that as the

Table 3
Volume of different components of the gas products.

Gas components	Gas volume (mL)			
	300 °C	400 °C	500 °C	600 °C
Hydrogen	0.01	0.06	0.54	6.39
Hydrogen sulfide	0.01	0.01	0.01	0.01
Methane	0.02	0.14	3.68	20.47
Ethane	0.11	0.14	1.86	9.47
Ethylene	0.02	0.10	1.36	15.24
Propane	0.56	0.55	1.14	2.93
Propylene	0.06	0.17	1.41	12.00
Iso-butane	0.19	0.18	0.14	0.26
N-butane	0.94	0.98	0.76	1.30
T-2-butene	0.01	0.02	0.14	2.47
1-butene	0.01	0.04	0.36	0.00
Isobutylene	0.02	0.03	0.25	1.83
C-2-butene	0.01	0.01	0.10	0.88
1,3-butadiene	0.00	0.00	0.05	0.00
Carbon monoxide	0.00	0.19	0.13	0.68
Carbon dioxide	0.17	0.50	4.80	1.22

temperature increases, the liquid product color changes from amber to dark brown color. This implies that the liquid product at low cracking temperature may be attributed to the light naphtha component of the feed that got distilled at the low temperature, leaving behind the sticky heavy liquid that stuck to the quartz wool. Consequently, the liquid product at low temperature will not contain heavy hydrocarbon since the temperature is not high enough to induce thermal cracking of the large molecular weight hydrocarbon (resin and asphaltene) and on the other hand, these heavy hydrocarbons could not be distilled as a liquid product. The observation agrees with the photograph and description of the SARA fractions reported in other studies [30,31]. However, the condensed liquid collected at temperatures above 400 °C seems to contain relatively large molecular weight hydrocarbons while at 400 °C and 300 °C the product's color reflects the absence of resin and asphaltene in their content.

SARA analysis was conducted for all collected condensed liquid products obtained under different pyrolysis temperatures to evaluate the distribution of saturates, aromatics, resins, and asphaltene. According to Fig. 6, the proportion of the saturates fractions exhibits a general trend of gradual decrease with increasing pyrolysis temperature but contrarily, increasing temperature induces gradual increase of aromatics fractions. However, a sudden decrease in aromatics fractions at 500 °C was observed before it resumed increasing above 500 °C. Referring to various studies, the saturate/aromatics ratio of crude oil is usually reported as a maturity indicator that reflects the relative thermal stability of saturates to aromatics [32]. This decreasing trend indicates the lower thermal stability of saturates to aromatics. In agreement with the results of this study, some researchers found that saturate and aromatics are more stable than asphaltene and resin [33]. At higher temperatures, the appearance of resin fractions in the pyrolyzed condensed liquid indicates that the boiling point of the resin is above 400 °C. Moreover, the increase in the resin proportions is attributed to more decomposition of asphaltene.

The elemental analysis was performed for condensed liquid products obtained at different pyrolysis temperatures. Results indicate the distribution of carbon and hydrogen among collected fractions of liquid. From Table 4 for pyrolysis temperature of 300 °C, we could see a negligible amount of nitrogen mostly captured at low temperatures from purging gas. Results also inferred a rich liquid hydrocarbon environment represented by carbon and hydrogen with a proportional molar ratio of 1:2, respectively. Our conclusions reveal that the liquid hydrocarbon environment collected at 300 °C consists of almost equal fractions of saturates and aromatics indicated by molar rations and further confirmed by SARA analysis. Increasing the pyrolysis temperature to 400 °C is appreciably increasing the amount of carbon with almost constant hydrogen content. This can be explained by an increase of unsaturated fractions as more carbon becomes hydrogen deficient and this is achieved through an increase of aromatics fraction. Consistent increment observed in carbon and hydrogen content with increasing temperatures up to 600 °C is due to the presence of the previously mentioned liquid hydrocarbon environment. At the same time, the slight increase in carbon content over hydrogen content is mainly due to an increase in unsaturated fractions and hydrogen-deficient carbon.

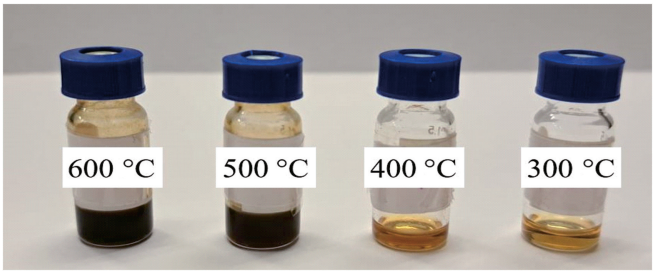

Fig. 5. Condensed liquid products at different pyrolysis temperatures.

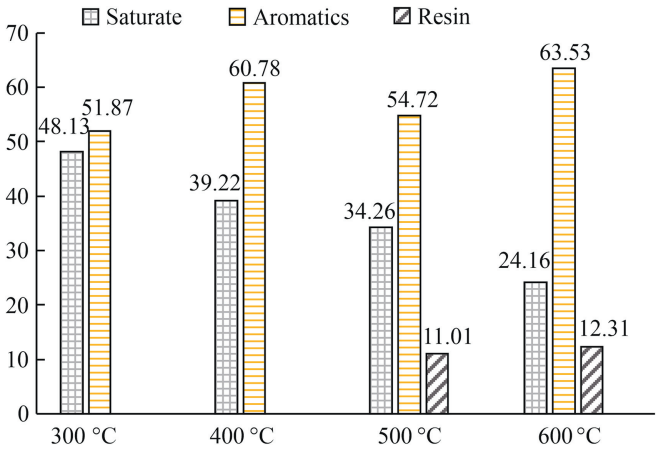

Fig. 6. SARA fractions of condensed liquid at different pyrolysis temperatures.

Table 4
Elemental analysis of liquid products of crude oil pyrolysis at different pyrolysis temperatures.

Pyrolysis temperature	Elemental composition (wt%)			
	C	H	N	S
300 °C	67.69	10.34	0.26	0
400 °C	76.57	10.46	0.09	0.30
500 °C	79.78	12.51	0	0.13
600 °C	82.02	12.02	0	0.43

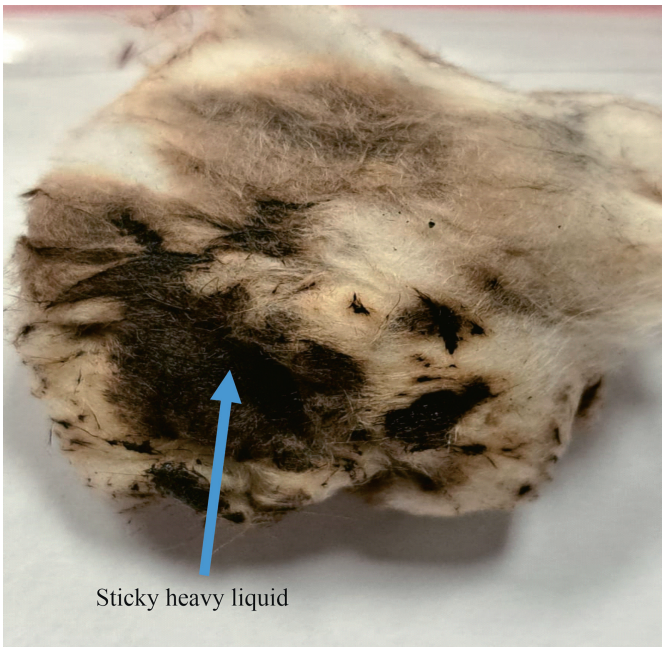

Fig. 7. Sticky heavy liquid deposited on top of quartz wool at low pyrolysis temperatures.

Table 5
SimDist for condensed liquid of crude oil pyrolysis at different pyrolysis temperatures.

Distillation products	Boiling points (°C)	Chemical composition [34]	wt%			
			300 °C	400 °C	500 °C	600 °C
Naphtha	0–221	Normal and iso-paraffins	45.3	39.2	42.0	37.1
Light cycle oil	221–343	Aromatics	37.0	32.6	30.4	34.5
Heavy cycle oil	>343	Heavy aromatics and NSO compounds	17.7	28.2	27.6	28.4
Aromatics[a]	>221	Aromatics and heavy aromatics	54.7	60.8	58.0	62.9

[a] Aromatics represents an introduced category calculated by the summation of light and heavy cycle oil percentages.

Fig. 7 depicts the sticky heavy liquid observed at low pyrolysis temperatures. The difficulty of sampling the sticky heavy liquid hindered further characterization. However, it is expected that the composition of the sticky heavy liquid mainly comprises the heavy fractions of oil. This expectation can be supported by their disappearance at high temperatures accompanied by coke appearance.

SimDist analysis has been employed for further classification of collected condensed liquid products. The components in collected liquid are measured and categorized according to their boiling points into naphtha, light cycle oil, and heavy cycle oil class. As shown in Table 5, the naphtha components percentage showed strong agreement with saturates measured in SARA analysis at low temperatures of 300 and 400 °C. While at high temperatures of 500 and 600 °C, SimDist results for saturates showed a higher percentage than that obtained in SARA analysis. This increase in saturates above 500 °C is due to the conversion of resins to light hydrocarbons. Aromatics were obtained in two classes; light and heavy cycle oil and the summation of their total percentage shows strong agreement with SARA results.

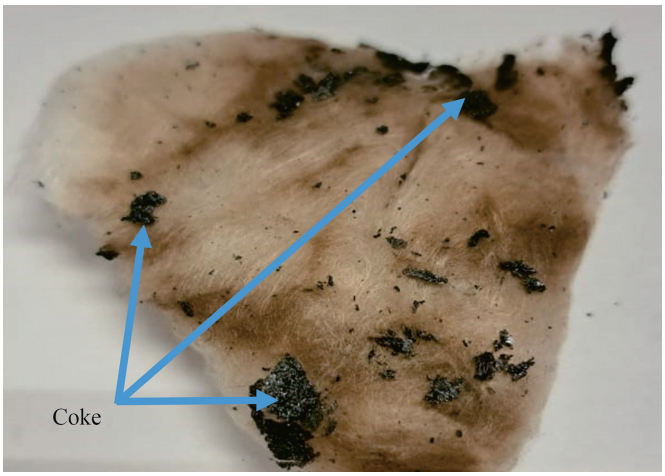

Fig. 8. Photograph of coke on the top of quartz wool observed at high pyrolysis temperatures.

3.1.3. Pyrolytic coke product

Pyrolytic coke product was observed in the crude oil pyrolysis at temperatures higher than 400 °C, and the yield reached the maximum at a pyrolysis temperature of 600 °C. Fig. 8 depicts the coke products on quartz wool.

It was observed that as the temperature increased the coking process increased and it reached the maximum at 600 °C whereas no coke deposition was observed at 400 °C and below. The formation of coke is attributed to the decomposition of asphaltene and resin. van der Waals attractive force induces the deposition of the aggregated asphaltene whereas during the process the hydrocarbon bonds break and form unsaturated hydrocarbons that later condense into coke [35]. Coke plays an important role in in-situ combustion gasification since it is considered the main fuel for the combustion front movement. Subsequently, the evaluation of the coke products formed by pyrolysis can help in improving field implementation of ISCG to enhance hydrogen generation. Fig. 9 illustrates the morphological characteristics of the pyrolyzed coke

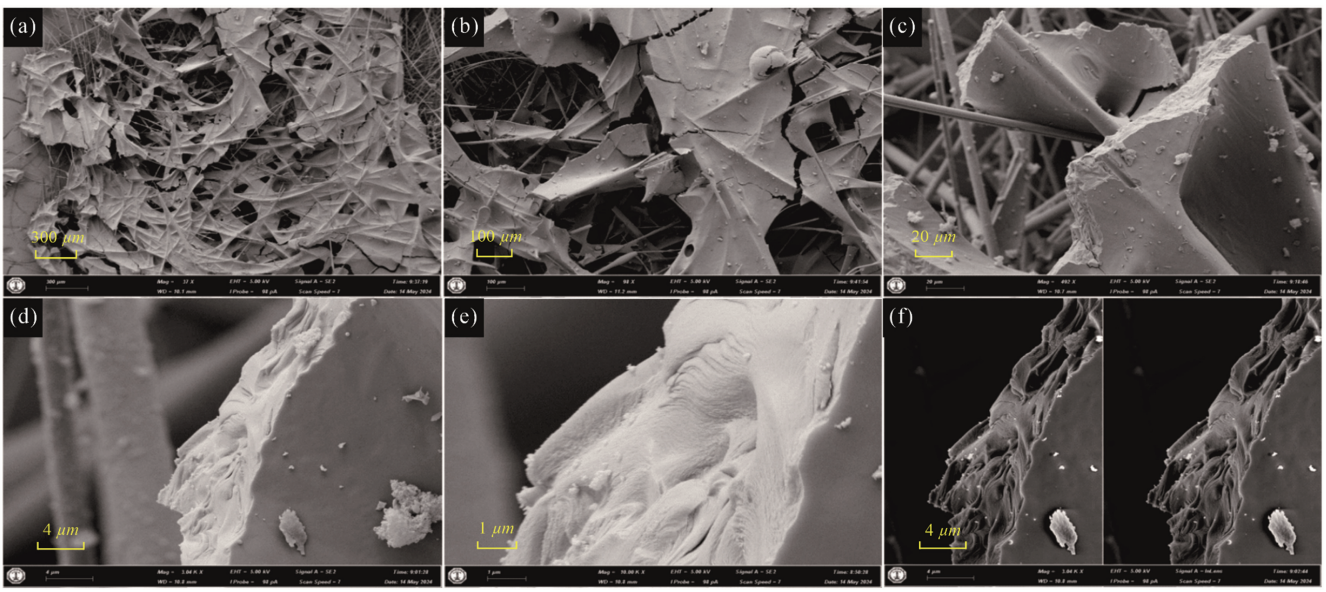

Fig. 9. SEM images of the deposited pyrolyzed coke.

Table 6
Elemental analysis of coke product at 600 °C.

Pyrolysis temperature	Elemental composition (wt%)			
	C	H	N	S
600 °C	78.79	2.21	0	9.4

product on top of the quartz wool. The morphological features of the pyrolyzed coke are similar to the transitional coke type that was reported by Chen et al. [36].

Fig. 9(a)–(c) shows the deposited coke on the quartz wool, the coke deposition is shown as a sheet of coke that covered the net-like morphology of the quartz wool rods. The images show that the surface of the coke is almost flat with few pores. The micro-crystalline structure of the coke has a wave-like structure as shown in Fig. 9(d)–(f). Also, in Fig. 9(c)–(f), white pellets with a coral-like morphology were generated on the top of the coke surface. Some studies reported the white pellets as secondary coke formed by volatiles [37], while other studies consider it as carbon aggregation caused by the condensation and dehydrogenation of heavy oil [38]. It can be concluded that the depicted coke with a flat surface and absence of pores inferred a worse combustion reactivity.

The elemental analysis of the pyrolyzed coke is listed in Table 6. The results show a high sulfur content as compared to that obtained in the condensed liquid products. This indicates that the coking process desulfurized the crude oil and absorbed most of the sulfur present in the original sample.

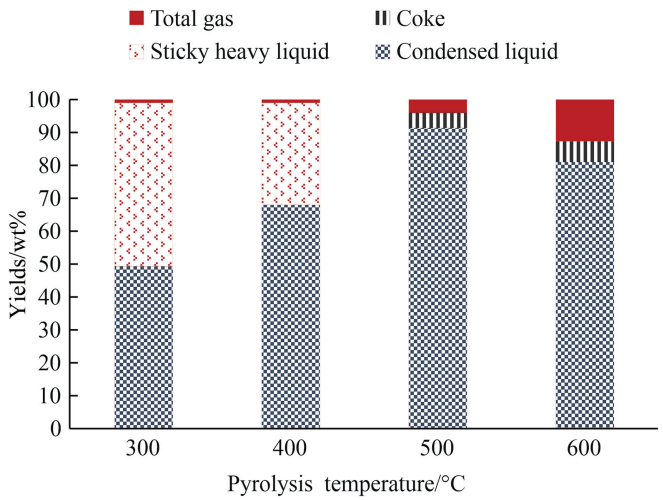

Fig. 10. Effect of sandstone on the pyrolytic products yield at different temperatures.

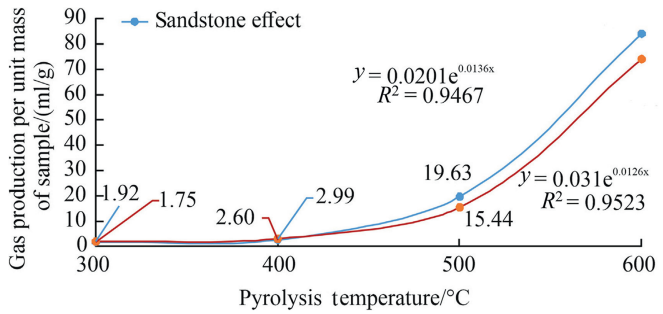

Fig. 11. Effect of sandstone on the gas yield per unit mass of the sample.

Table 7
Effect of the sandstone on the volume of the gas products.

Gas components	Gas volume (mL)			
	300 °C	400 °C	500 °C	600 °C
Hydrogen	0.01	0.02	1.71	8.15
Hydrogen sulfide	0.01	0.01	0.01	0.01
Methane	0.02	0.12	4.84	25.65
Ethane	0.10	0.15	2.35	12.15
Ethylene	0.02	0.06	1.46	19.07
Propane	0.56	0.60	1.19	3.79
Propylene	0.05	0.13	1.42	13.79
Iso-butane	0.00	0.19	0.11	0.28
N-butane	0.97	1.02	0.60	1.51
T-2-butene	0.00	0.02	0.00	0.98
1-Butene	0.01	0.03	0.10	3.55
Isobutylene	0.00	0.03	0.23	1.86
C-2-butene	0.01	0.01	0.07	0.69
1,3-Butadiene	0.00	0.00	0.05	0.00
Carbon monoxide	0.00	0.13	0.22	0.53
Carbon dioxide	0.18	0.44	6.12	1.82

3.2. Effect of the presence of sandstone

The effect of sandstone on the generated gases during pyrolysis is suspected to be attributed to the clay minerals present in the rock. Researchers have investigated the effect of heat on clay minerals in sandstone, and they found that some clay minerals experienced conversion to other clay minerals while others collapsed and disappeared [39]. However, the transformation of α-quartz to β-quartz was observed at temperatures of 580–595 °C. Another observation is the complete collapse of kaolinite at 550 °C, while, illite loses structural water at 553 °C.

In this study, the effect of sandstone mineralogy was investigated by placing 5 g of dried crushed sandstone on top of the quartz wool at the bottom of the reactor. The experiments were conducted in a temperature range of (300–600 °C) for a residence time of 8 min. Fig. 10 shows the product yield in each experiment where the sandstone mineralogy influences the products. At a temperature of 300 and 400 °C, no noticeable change is observed in the product yields as compared with the results for crude oil pyrolysis without sandstone. This inferred that the adsorptive and catalytic effect of the clay minerals is pronounced at higher temperatures. It is believed that clays catalyze the pyrolysis reaction either by donating hydrogen cation (Brønsted) or by accepting an electron pair (Lewis acid sites). At 500 °C, slight thermal alteration occurred, except that there is a slight increase in the total gas yield (1.04 wt% instead of 0.59 wt% without sandstone). The increase in the gas yields is attributed to the catalytic effect of the clay minerals, which causes enhancement in hydrocarbon cyclization and isomerization that leads to light hydrocarbon generation. With the increase in

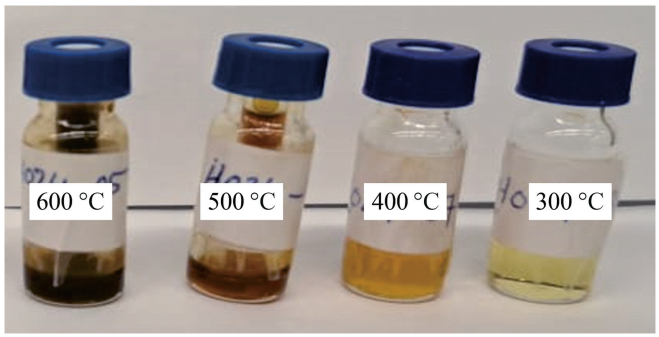

Fig. 12. Effect of sandstone on condensed liquid at different pyrolysis temperatures.

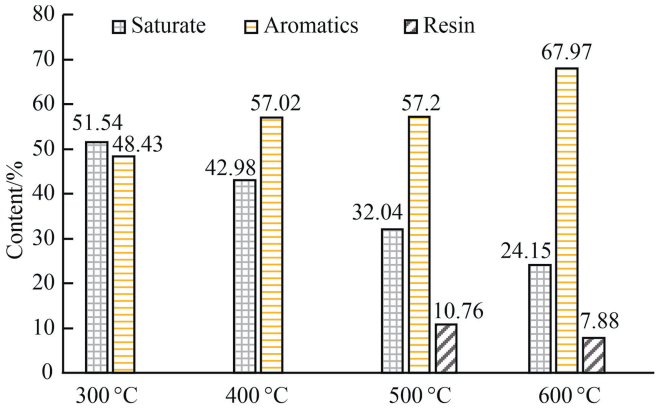

Fig. 13. Effect of sandstone SARA fractions of condensed liquid at different pyrolysis temperatures.

Table 8
Elemental analysis of liquid products of crude oil pyrolysis in the presence of sandstone at different pyrolysis temperatures.

Pyrolysis Temperature	Elemental composition (wt%)			
	C	H	N	S
300 °C	67.33	10.33	0.55	0
400 °C	69.49	10.42	0.02	0.15
500 °C	77.84	11.19	0.02	0.77
600 °C	86.66	12.34	0	0.24

temperature up to 600 °C, the crude oil pyrolysis rate increases, resulting in enhancement in gas yields and reduction in coke yield.

3.2.1. Effect of sandstone on the pyrolytic gas product

Fig. 11 shows the total gas produced at each experiment. It was observed that the sandstone addition enhanced the total volume of the gases produced at each temperature and the volume increased with the increase in temperature. It was observed that the catalytic effect of clay minerals is more active at higher temperatures.

An exponential increase in the total volume of gaseous products was observed with increasing temperature starting from 1.75 mL/g at 300 °C to a maximum value of 84.06 mL/g at 600 °C. Several studies [40,41] have investigated the effect of clay minerals on the various products formed during oil pyrolysis.

The change in volume of the generated gas components as a function of the pyrolysis temperature and the addition of dried crushed sandstone is detailed in Table 7. It can be observed that the effect of the sandstone occurred at temperatures above 400 °C. The clear enhancement in the methane, ethylene, propylene, ethane, and hydrogen percentages compared to their percentages in the experiments conducted without sandstone infer the catalytic effects of clay minerals on the enhancement of light hydrocarbons at high temperatures.

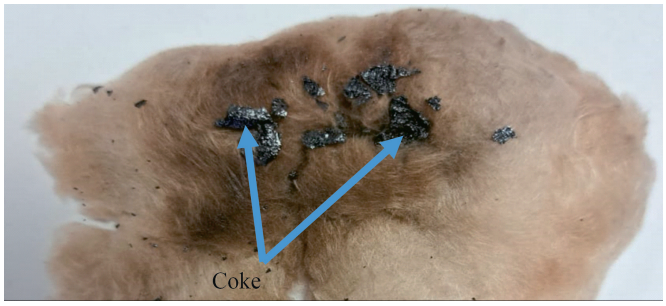

Fig. 14. Photograph of coke on the top of quartz wool.

3.2.2. Effect of sandstone on the pyrolytic liquid product

Fig. 12 shows the effect of sandstone on the condensed liquid products at pyrolysis temperatures in the range of 300–600 °C. The color of condensed liquid products was not affected by the presence of the sandstone, whereas a similar color-changing trend with temperature was observed.

The SARA analysis of condensed liquid products of the crude oil pyrolysis in the presence of sandstone is shown in Fig. 13. This trend has similarities to that of crude oil pyrolysis without sandstone, except that at high temperatures, a clear increase in aromatic fractions and a decrease in resin fractions is observed. This is attributed to the catalytic activity of clays at high temperatures. It has been reported that the high adsorption capacity of kaolinite and illite improves the decomposition of heavy unstable hydrocarbons and causes the formation of light stable aromatic compounds [42].

The elemental analysis of the condensed liquid products measured at different pyrolysis temperatures is listed in Table 8. At low temperatures, the elemental composition of condensed liquid from crude oil pyrolysis in the absence of sandstone and the presence of sandstone is nearly the same, signaling less effect of sandstone. However, as the temperature increases changes in the percentage of carbon and hydrogen were observed. This observation can be linked with the increase in aromatics measured by SARA analysis.

The percentages of the three categories of distillation products analyzed at different temperatures are listed in Table 9. There is an agreement between the SimDist results and SARA results measured at low temperatures, while variations are observed at high temperatures. This difference in results at high temperatures is attributed to the appearance of resin.

3.2.3. Effect of sandstone on the pyrolytic coke product

Fig. 14 shows the pyrolytic coke product deposited on the quartz wool in the experiment conducted with the presence of sandstone.

Similar to the coke produced in the experiment without sandstone, the coking process observed with the presence of sandstone also increased as the temperature increased, and it reached the maximum at 600 °C, whereas no coke was deposited at 400 °C and below. The coke deposited on the quartz wool during the crude oil pyrolysis in the presence of sandstone looks denser than the coke deposited in the absence of the sandstone. Also, it was observed

Table 9
Effect of sandstone on SimDist for condensed liquid of crude oil pyrolysis at different pyrolysis temperatures.

Distillation products	Boiling points (°C)	Chemical composition [34]	wt%			
			300 °C	400 °C	500 °C	600 °C
Naphtha	0–221	Normal and iso-paraffins	47	42.5	39.8	45.2
Light cycle oil	221–343	Aromatics	36.5	32.9	29.8	29.1
Heavy cycle oil	>343	Heavy aromatics and NSO compounds	16.5	24.6	30.4	25.7
Aromatics[a]	>221	Aromatics and heavy aromatics	53	57.5	60.2	54.8

[a] Aromatics represents an introduced category calculated by the summation of light and heavy cycle oil percentages.

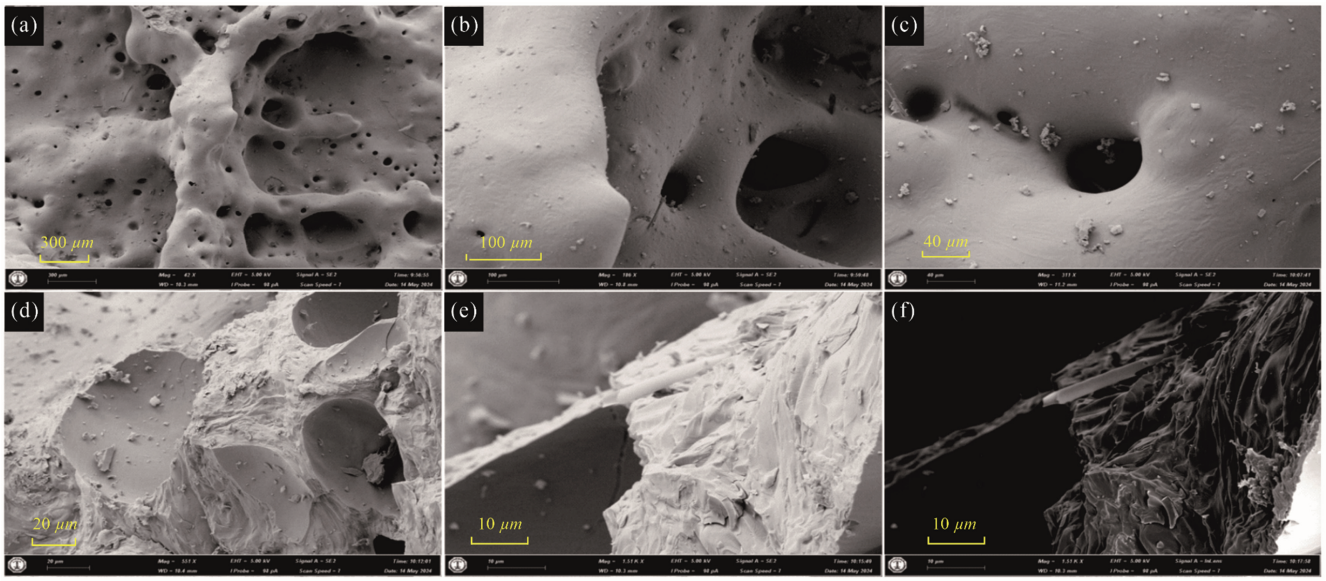

Fig. 15. SEM images of deposited pyrolyzed coke.

Table 10
Elemental analysis of coke product for crude oil pyrolysis in the presence of sandstone at 600 °C.

Pyrolysis Temperature	Elemental composition (wt%)			
	C	H	N	S
600 °C	75.03	2.66	0	7.91

that coke deposition was within a confined area and not dispersed as observed during crude oil pyrolysis without sandstone. The morphological characteristics of the deposited pyrolyzed coke on top of the quartz wool are illustrated in Fig. 15.

The morphology of the pyrolyzed coke is similar to the transitional coke type reported by Chen et al. [36]. As seen in Fig. 15(a), the surface of the coke has the form of a flat surface with wrinkles and pores of different sizes disseminated in the coke surface. Also, some pores are interconnected. Various sizes of pores that covered the whole coke area with the presence of the white pellets on the coke surface are shown in Fig. 15(b) and 15(c). Microcrystalline structure of threadlike morphology was observed in Fig. 15(d)–(f). It was concluded that the evolution of gases from the pyrolyzed sandstone due to alteration or vaporization of some components of clay at high temperatures led to pores creation on the coke surface. The observations indicate that coke has better combustion reactivity due to the existence of interconnected pores.

The elemental analysis of the pyrolyzed coke is listed in Table 10. Compared to the elemental analysis of coke produced by the experiment without sandstone, the result shows a reduction in all elements. This can be attributed to the released gases that create pores in the coke surface and thus decrease the specific surface area of the coke. The reduction of surface area reduces the adsorption capacity of the coke.

4. Conclusions

This study demonstrates the potential for direct hydrogen production from oil reservoirs. The role of pyrolysis in in-situ hydrogen generation from crude oil was investigated using a fixed-bed micro-activity test (MAT) unit. Pyrolysis experiments were conducted in the temperature range of 300–600 °C and under atmospheric pressure. The primary conclusions drawn from the study are as follows:

(1) The distribution of the products from crude oil pyrolysis depends mainly on the temperature.
(2) In the absence of sandstone, the volume of hydrogen generated was 6.39 mL at a pyrolysis temperature of 600 °C, whereas the presence of sandstone enhanced the hydrogen generation, reaching a maximum volume of 8.15 ml at 600 °C.
(3) Coke deposition was first observed at a pyrolysis temperature of 500 °C, with the yield increasing to a maximum at 600 °C.
(4) The deposition of sticky heavy liquid was observed at lower temperatures, while higher temperatures led to the formation of coke and the disappearance of sticky heavy liquid. This may indicate that the sticky heavy liquid partially or completely converts to coke at higher temperatures.
(5) This study demonstrated the contribution of the pyrolysis reaction to in-situ hydrogen generation and quantitatively and qualitatively assessed the pyrolysis products. Additionally, it confirmed the catalytic effect of sandstone in enhancing hydrogen generation. The results provide valuable insights that could be useful for the development of kinetic models. Future work could explore various gasification reactions, such as aqua-thermolysis and partial oxidation, to provide comprehensive information for core flooding experiments under various reservoir conditions.

CRediT authorship contribution statement

Mohamed Abdalsalam Hanfi: Writing – review & editing, Writing – original draft, Methodology, Investigation, Formal analysis, Data curation, Conceptualization. **Olalekan Saheed Alade:** Writing – review & editing, Validation, Resources, Project administration, Methodology, Conceptualization. **Abdulkadir Tanimu:** Writing – review & editing, Validation, Supervision, Resources, Methodology, Investigation. **Mohamed Mahmoud:** Writing – review & editing, Supervision, Project administration, Methodology, Funding acquisition, Conceptualization. **Sulaiman A. Alarifi:**

Writing – review & editing, Validation, Supervision, Project administration, Methodology, Conceptualization.

Declaration of competing interest

The authors declare that they have no known competing financial interests or personal relationships that could have appeared to influence the work reported in this paper.

Acknowledgment

The authors would like to acknowledge the support of the College of Petroleum Engineering & Geosciences at King Fahd University of Petroleum & Minerals (KFUPM) and Mr. Ramzi Hadi Al-Shuqaih of the Interdisciplinary Research Center for Refining and Advanced Chemicals at KFUPM.

References

[1] A. T-Raissi, D.L. Block, Hydrogen: automotive fuel of the future, IEEE Power Energy Mag. 2 (2004) 40–45.
[2] M. Yu, K. Wang, H. Vredenburg, Insights into low-carbon hydrogen production methods: green, blue and aqua hydrogen, Int. J. Hydrogen Energy 46 (2021) 21261–21273.
[3] IEA, Global Hydrogen Review 2023, 2023.
[4] N. Muradov, Low to near-zero CO2 production of hydrogen from fossil fuels: status and perspectives, Int. J. Hydrogen Energy 42 (2017) 14058–14088.
[5] P. Song, Y. Li, Z. Yin, M.A. Ifticene, Q. Yuan, Simulation of hydrogen generation via in-situ combustion gasification of heavy oil, Int. J. Hydrogen Energy 49 (2024) 925–936.
[6] P. Song, Y. Li, Z. Yin, Q. Yuan, Hydrogen Generation from Heavy Oils via In-Situ Combustion Gasification. SPE Western Regional Meeting, SPE, 2023. D031S007R003.
[7] P.R. Kapadia, M.S. Kallos, I.D. Gates, Potential for hydrogen generation from in situ combustion of Athabasca bitumen, Fuel 90 (2011) 2254–2265.
[8] H.A.-H. Ibrahim, Recent Advances in Pyrolysis, BoD–Books on Demand, 2020.
[9] P. Liu, M. Zhu, Z. Zhang, D. Zhang, Pyrolysis of an Indonesian oil sand in a thermogravimetric analyser and a fixed-bed reactor, J. Anal. Appl. Pyrolysis 117 (2016) 191–198.
[10] R. Zhao, T. Wang, H. Ren, N. Jiang, X. Li, W. Lv, et al., A strategy for enhanced hydrogen generation: the effect of varying atmospheres on in-situ gasification in heavy oil reservoirs, Appl. Energy 376 (2024) 124168.
[11] M.A. Ifticene, Q. Yuan, Mechanisms of hydrogen generation during in-situ combustion gasification of heavy oil, SPE Western Regional Meeting, SPE (2024). D021S011R005.
[12] J.G. Speight, Thermal cracking of Athabasca bitumen, Athabasca asphaltenes, and Athabasca deasphalted heavy oil, Fuel 49 (1970) 134–145.
[13] D. Liu, Q. Song, J. Tang, R. Zheng, Q. Yao, Interaction between saturates, aromatics and resins during pyrolysis and oxidation of heavy oil, J. Pet. Sci. Eng. 154 (2017) 543–550.
[14] S. Yang, S. Huang, Q. Jiang, C. Yu, X. Zhou, Experimental study of hydrogen generation from in-situ heavy oil gasification, Fuel 313 (2022) 122640.
[15] X. Tang, W. Pu, Q. Chen, R. Liu, Y. Yang, An experimental investigation on hydrogen generation from in-situ gasification by pyrolysis, Int. J. Hydrogen Energy 49 (2024) 1019–1027.
[16] H. He, Q. Li, J. Tang, P. Liu, H. Zheng, F. Zhao, et al., Study of hydrogen generation from heavy oil gasification based on ramped temperature oxidation experiments, Int. J. Hydrogen Energy 48 (2023) 2161–2170.
[17] Q. Yuan, X. Jie, B. Ren, Hydrogen generation in crushed rocks saturated by crude oil and water using microwave heating, Int. J. Hydrogen Energy 47 (2022) 20793–20802.
[18] B.M. Storey, R.H. Worden, D.D. McNamara, The geoscience of in-situ combustion and high-pressure air injection, Geosciences 12 (2022) 340.
[19] S.P. Choquette, S. Krishnaswamy, P.S. Northrop, J.T. Edwards, L. Hooman, R. Bret, et al., Esperson Dome oxygen combustion pilot test: postburn coring results, SPE Reserv. Eng. 8 (1993) 85–93.
[20] J. Sharma, J. Dean, F. Aljaberi, N. Altememee, In-situ combustion in Bellevue field in Louisiana–History, current state and future strategies, Fuel 284 (2021) 118992.
[21] S. Huang, J.J. Sheng, An innovative method to build a comprehensive kinetic model for air injection using TGA/DSC experiments, Fuel 210 (2017) 98–106.
[22] C. Yuan, D.A. Emelianov, M.A. Varfolomeev, Oxidation behavior and kinetics of light, medium, and heavy crude oils characterized by thermogravimetry coupled with fourier transform infrared spectroscopy, Energy Fuels 32 (2018) 5571–5580.
[23] C. Yuan, M.A. Varfolomeev, D.A. Emelianov, A.A. Eskin, R.N. Nagrimanov, M.V. Kok, et al., Oxidation behavior of light crude oil and its SARA fractions characterized by TG and DSC techniques: differences and connections, Energy Fuels 32 (2018) 801–808.
[24] Y. Qi, C.-F. Cai, P. Sun, D.-W. Wang, H.-J. Zhu, Crude oil cracking in deep reservoirs: a review of the controlling factors and estimation methods, Pet. Sci. 20 (2023) 1978–1997.
[25] M.L.A. Gonçalves, D.A. Ribeiro, A.M.R.F. Teixeira, M.A.G. Teixeira, Influence of asphaltenes on coke formation during the thermal cracking of different Brazilian distillation residues, Fuel 86 (2007) 619–623.
[26] P.R. Kapadia, M.S. Kallos, I.D. Gates, A new kinetic model for pyrolysis of Athabasca bitumen, Can. J. Chem. Eng. 91 (2013) 889–901.
[27] M.R. Gray, Upgrading Oilsands Bitumen and Heavy Oil, University of Alberta, 2015.
[28] Y. Che, Z. Yang, Y. Qiao, J. Zhang, Y. Tian, Study on pyrolysis characteristics and kinetics of vacuum residue and its eight group-fractions by TG-FTIR, Thermochim. Acta 669 (2018) 149–155.
[29] K. Wakui, K. Satoh, G. Sawada, K. Shiozawa, K. Matano, K. Suzuki, et al., Dehydrogenative cracking of n-butane using double-stage reaction, Appl. Catal. Gen. 230 (2002) 195–202.
[30] S. Rudyk, Relationships between SARA fractions of conventional oil, heavy oil, natural bitumen and residues, Fuel 216 (2018) 330–340.
[31] J.W. Park, M.Y. Kim, S.I. Im, K.S. Go, N.S. Nho, K.B. Lee, Development of correlations between deasphalted oil yield and Hansen solubility parameters of heavy oil SARA fractions for solvent deasphalting extraction, J. Ind. Eng. Chem. 107 (2022) 456–465.
[32] P.C. Hackley, T.M. Parris, C.F. Eble, S.F. Greb, D.C. Harris, Oil–source correlation studies in the shallow Berea Sandstone petroleum system, eastern Kentucky, Am. Assoc. Petrol. Geol. Bull. 105 (2021) 517–542.
[33] A. Boytsova, N. Kondrasheva, J. Ancheyta, Thermogravimetric determination and pyrolysis thermodynamic parameters of heavy oils and asphaltenes, Energy Fuels 31 (2017) 10566–10575.
[34] P. Behrenbruch, T. Dedigama, Classification and characterisation of crude oils based on distillation properties, J. Pet. Sci. Eng. 57 (2007) 166–180.
[35] J.S. Buckley, Asphaltene deposition, Energy Fuels 26 (2012) 4086–4090.
[36] K. Chen, H. Zhang, U.-K. Ibrahim, W. Xue, H. Liu, A. Guo, The quantitative assessment of coke morphology based on the Raman spectroscopic characterization of serial petroleum cokes, Fuel 246 (2019) 60–68.
[37] J. Guo, Y. Li, B. Wang, T. Zhu, Carbon consumption mechanism of activated coke in the presence of water vapor, Environ. Sci. Pollut. Control Ser. 27 (2020) 1558–1568.
[38] J.-X. Wang, L.-L. Wang, T.-F. Wang, W.-F. Pu, Exothermal property and kinetics analysis of oxidized coke and pyrolyzed coke from Fengcheng extra-heavy oil, Ind. Eng. Chem. Res. 60 (2021) 7014–7023.
[39] A. Torok, M. Hajpál, Effect of temperature changes on the mineralogy and physical properties of sandstones. A laboratory study, Int. J. Restor. Build. Monum. 11 (2005) 211.
[40] C. Pan, L. Jiang, J. Liu, S. Zhang, G. Zhu, The effects of pyrobitumen on oil cracking in confined pyrolysis experiments, Org. Geochem. 45 (2012) 29–47.
[41] M. He, Z. Wang, M.J. Moldowan, K. Peters, Insights into catalytic effects of clay minerals on hydrocarbon composition of generated liquid products during oil cracking from laboratory pyrolysis experiments, Org. Geochem. 163 (2022) 104331.
[42] T. Li, C. Wu, Research on the abnormal isothermal adsorption of shale, Energy Fuels 29 (2015) 634–640.